Article:
Tangparitkul, S, Jiang, J, Jeraal, M et al. (2 more authors) (2023) Competitive Adsorption of Interfacially Active Nanoparticles and Anionic Surfactant at the Crude Oil–Water Interface. Langmuir, 39 (7). pp. 2483-2490. ISSN 0743-7463

https://doi.org/10.1021/acs.langmuir.2c01413

Competitive Adsorption of Interfacially Active Nanoparticles and Anionic Surfactant at the Crude Oil-Water Interface

Suparit Tangparitkul[1,*], Jiatong Jiang[2], Mohammed Jeraal[3],

Thibaut V.J. Charpentier[4] and David Harbottle[2]

[1]Department of Mining and Petroleum Engineering, Faculty of Engineering, Chiang Mai University, Chiang Mai, 50200, Thailand
[2]School of Chemical and Process Engineering, University of Leeds, Leeds, LS2 9JT, United Kingdom
[3]Cambridge Centre for Advanced Research and Education in Singapore Ltd., 1 Create Way, CREATE Tower #05-05, 138602, Singapore
[4]Baker Hughes, Oilfield Services, Liverpool, L33 7SY, United Kingdom
*To whom correspondence should be addressed. Email: suparit.t@cmu.ac.th (S.T.)

Abstract

The interfacial activity of poly(N-isopropylacrylamide) (pNIPAM) nanoparticles in the absence and presence of an anionic surfactant (sodium dodecyl sulfate, SDS) was studied at a crude oil-water interface. Both species are interfacially active and can lower the interfacial tension, but when mixed together, the interfacial composition was found to depend on the aging time and total component concentration. With the total component concentration less than 0.0050 wt%, the reduced interfacial tension by pNIPAM was greater than SDS, thus pNIPAM has a greater affinity to partition at the crude oil-water interface. However, the lower molecular weight (smaller molecule) of SDS compared to pNIPAM meant that it rapidly partitioned at the oil-water interface. When mixed, the interfacial composition was more SDS-like for low total component concentrations ($\leq$ 0.0010 wt%), while above, the interfacial composition was more pNIPAM-like, similar to the single component response. Applying a weighted-arithmetic mean approach, the surface-active contribution (%) could be approximated for each component, pNIPAM and SDS. Even though SDS rapidly partitioned at the oil-water interface, it was shown to be displaced by the pNIPAM nanoparticles, and for the highest total component concentration, pNIPAM nanoparticles were predominantly contributing to the reduced oil-water interfacial tension. These findings have implications into the design and performance of fluids that are used to enhance crude oil production from reservoirs, particularly highlighting the aging time and component concentration effects to modify interfacial tensions.

Introduction

Nanoparticles are being trialed in the field to enhance crude oil recovery having been widely reported to improve oil displacement, although the governing mechanisms for this enhancement remains to be debated.[1-4] Interfacial and surface forces undoubtedly contribute to oil displacement, with nanoparticles modifying both the interfacial (oil-water) and surface (oil-water-solid) properties.[3-5] The structural disjoining pressure from accumulating nanoparticles in the "liquid-wedge" between the substrate and droplet has been highlighted as a mechanism to displace oil films in the absence of other chemical additives.[1, 6-7] Furthermore, nanoparticles can be deployed to improve sweep efficiency by increasing the viscosity of the injected fluid, although this phenomena is outside the scope of the current study. What is the focus is the dual effect of nanoparticles and surfactants competing at oil-water interfaces, something that is rarely studied but is of significant practical importance in the design of nanofluids for enhanced oil recovery (EOR).

Co-adding surfactants and nanoparticles to EOR fluids should be favorable as the two components can promote greater displacement of an oil-wetted film on a substrate.[1] Surfactants contribute by mainly lowering the oil-water interfacial energy σ_{OW}, changing the balance of the three interfacial energies (σ_{OW}, σ_{OS} and σ_{SW}) that govern the equilibrium contact angle (θ) of the oil on the reservoir rock; and nanoparticles contribute by increasing the disjoining pressure between the oil and rock surface, but can also modify the substrate wettability to become more hydrophilic, thus making it more favorable for the oil to dewet the reservoir rock.[4, 8-9]

While the loss of surfactant in the field is an environmental concern,[10] its recovery in the process fluid also creates challenges to the effectiveness of downstream processes. Using nanoparticles would be more favorable, but particularly the use of nanoparticles that exhibit controllable interfacial activity. Recently, the use of microgel particles for EOR has received attention because of their ability to readily partition at an oil-water interface,[11-12] thus lowering the surfactant demand for oil displacement. Furthermore, Ni et al.[13] showed that by using thermally-responsive microgels that partition at the oil-water interface, a crude oil-in-water emulsion could be rapidly destabilized by decreasing the temperature below the lower critical solution temperature (LCST) of the microgel, potentially alleviating some of the downstream processing difficulties. Currently, when used in the field both surfactants and nanoparticles are injected, and so it is important to understand the contributions of each to modifying interfacial properties.

Much of the literature considers oxide-based particles when studying the competitive adsorption between nanoparticles and surfactants. For example, Pichot et al.[14] showed that when co-adding Tween 60, a non-ionic surfactant, and nanosilica (Aerosil 200) to the aqueous phase, both species would partition at the oil-water interface at low surfactant concentration, but the interface was predominantly surfactant-loaded at high surfactant concentration. The authors speculated that at low surfactant concentration, surfactant adsorption onto the nanoparticles had depleted the surfactant concentration, hence the nanoparticles were able to partition at the oil-water interface.

Surfactant depletion was also shown by Ravera et al.[15] when studying CTAB, a cationic surfactant, and silica nanoparticles (Levasil). Using a fixed surfactant concentration (8×10^{-4} M), the authors proved that for silica concentrations > 0.4 wt%, almost all surfactants had been depleted due to adsorption onto silica, hence the reduction in interfacial tension was attributed to the nanoparticles, with the interfacial activity of the nanoparticles enhanced by the apparent increase in hydrophobicity following surfactant adsorption. Furthermore, when both particles and surfactants resided at the interface, the authors suggested that the long-time dynamics may result from a redistribution of surfactant between the solid-liquid and liquid-liquid interfaces.

Interestingly, when both surfactant and nanoparticles are dispersed in contrasting fluid phases, the surfactant wins-out and prevents nanoparticle adsorption at the oil-water interface.[16, 14] Such behavior, along with the sensitivity to the component concentrations, highlights the challenges associated with the design of EOR fluids to deliver optimal performance.

While most oxide-based nanoparticles are weakly interfacially active, unless hydrophobically modified, polymeric nanoparticles such as pNIPAM are not. These nanoparticles have been shown to substantially lower the interfacial tension (σ) by more than 30 mN/m,[17-19] and they are known to be good emulsion stabilizers. However, their competition at liquid-liquid interface in a dual component fluid is less well understood. In the current study, the interfacial activity of pNIPAM is measured in the absence and presence of an anionic surfactant, sodium dodecyl sulfate (SDS).

Materials and Experimental Methods

Materials. Heavy crude oil with a density of 946 kg/m^3 (18.03° API) (measured using a DMA 4200M, Anton Paar, UK) and viscosity of 363.7 mPa·s (measured using a DHR-2, TA Instruments, USA) at 60 °C was used throughout the study. The saturate, aromatic, resin and

asphaltene (SARA) content (by mass) and total acid number (TAN) of the heavy crude oil are summarized in Table 1. Prior to each test, the crude oil was shaken and de-gassed. SDS (Sigma-Aldrich), N-isopropylacrylamide (NIPAM, Sigma-Aldrich), N,N' Methylenebisacrylamide (BA, Fluka) and potassium persulfate (KPS, Merck) were used as received and without further purification. Ultrapure Milli-Q water was used in all experiments with a resistivity of 18.2 MΩ·cm and pH of 5.5.

Table 1. Chemical properties of the heavy crude oil.

SARA analysis (IP 469)			
Saturate	Aromatic	Resin	Asphaltene
7.4%	37.8%	15.3%	39.5%
TAN (ASTM D664)			
0.134 mg KOH/g			

Nanoparticle synthesis and characterization. The pNIPAM nanoparticles were synthesized following the method of Li et al.[17, 20] NIPAM (2.25 g) was dissolved in 250 mL Milli-Q water in a 500 mL three-necked flask. BA (75 mg) was added to the Milli-Q water and nitrogen bubbled through the solution for 30 min while being continuously stirred at 300 rpm. The solution temperature was raised to 70 °C using a thermostatically-controlled aluminum heating block and held for a further 30 min. During this time, KPS (0.25 g) was dissolved in 10 mL of Milli-Q water and degassed using nitrogen. The solution was then added dropwise to initiate the reaction via a gas-tight syringe. The reaction was left to polymerize at 70 °C for 3.5 h. The resulting dispersion was passed through glass wool to remove any agglomerated material and then further purified 5 times by centrifugation at 10,000 rpm. The synthesized pNIPAM was used as nanoparticles throughout the study. The stock solution of pNIPAM (prepared to 0.058 wt%) was diluted to the desired concentration before each use.

The hydrodynamic diameter and zeta potential of pNIPAM particles were measured using a ZetaSizer Nano ZS (Malvern Instrument, UK), with the fluid temperature varied from 20 to 65 °C. The temperature was controlled to within 1 °C and the dispersion was left to stabilize for 10 min at temperature prior to measurement. All particle size measurements were repeated at least 3 times and zeta potentials were an average of 12 measurements.

Preparation of nanofluids. The pNIPAM + SDS blend was prepared by mixing pNIPAM and SDS at an equivalent mass ratio, i.e. 1:1. Hence, the total component concentration remains

unchanged, but for the individual components (pNIPAM and SDS) their concentration is diluted by a factor of 2. To prepare the nanofluids, the pNIPAM dispersion was added to the SDS solution under gentle agitation and then mixed for 30 min to ensure good mixing. Fresh solutions were prepared and sonicated for 5 min prior to each use. It should be noted that the SDS concentrations used in the current study (≤ 0.0050 wt%) were below the critical micelle concentration (cmc) of SDS, c.a. 0.1 wt%, hence, no micelles would be present in the nanofluids.

Oil-water interfacial tension measurement. The interfacial tension of heavy crude oil-water was measured using a Theta Optical Tensiometer (Attension®, Biolin Scientific, Finland) equipped with a thermal cell (C217W, Biolin Scientific, Finland) and the temperature monitored using a k-type thermocouple (TC-08 data logger, Pico Technology, UK). A stainless inverted needle (Gauge 22) with a 1 mL gas-tight syringe (Hamilton Co., USA) was filled with 1 mL of crude oil and submerged in the aqueous solution at the desired temperature for 10 min to ensure the needle and crude oil were at the desired experimental temperature of 60 °C. The oil droplet was subsequently discharged from the needle using a micro-syringe pump (C201, Biolin Scientific, Finland) to instantaneously form a 10 µL droplet. The droplet shape profile was recorded dynamically at a frame rate of 2 fps to capture the dynamics of interfacial tension as surface-active species partition at the oil-water interface. The measurement was stopped when steady state had been reached (≤ 4,000 s), which was taken to be when the change in interfacial tension was less than 1 mN/m per 10 min. The interfacial tension was determined by the edge-detection method and fitted to the Young-Laplace equation.[21]

Results and Discussion

Nanoparticle characterization. Figure 1a shows the thermal response of the pNIPAM particles and mixtures of pNIPAM + SDS as the temperature is increased from 20 °C (temperature below the LCST) to 65 °C (temperature above the LCST). For pNIPAM in Milli-Q water, the particle hydrodynamic diameter decreased from ~225 nm at 20 °C to ~152 nm as the temperature approached the LCST (30 °C), and then above the LCST the particle diameter was ~55 nm and remained unchanged at higher temperatures. Based on the sizing data, the LCST was found to be between ~32 and 35 °C, which is in good agreement with the LCST values reported in the literature.[20, 22-23]

It has been shown that SDS binds to pNIPAM chains via hydrophobic interactions to increase the LCST of pNIPAM.[24-25] However, with the low surfactant concentrations used in the current study (i.e. $< 2 \times 10^{-2}$ wt%, which is significantly below the cmc), the effect of SDS modifying the LCST of pNIPAM is negligible, unlike its effect on the particle size which is seen below the LCST (Fig. 1).

Below the LCST, the hydrodynamic diameter of pNIPAM decreased with increasing SDS concentration, with the effect attributed to improved dispersibility (de-aggregation of larger clusters) of the pNIPAM particles induced by the anionic SDS.[26-27] However, above the LCST the effect of surfactant concentration is less significant, although the particle size with surfactant added is smaller than without surfactant, possibly due to the slightly higher ionic concentration (residual Na-ions) of the surfactant solution leading to a subtle collapse of the globule structure, see Fig. S1 in the Supporting Information which confirms an increase in solution conductivity with added SDS.

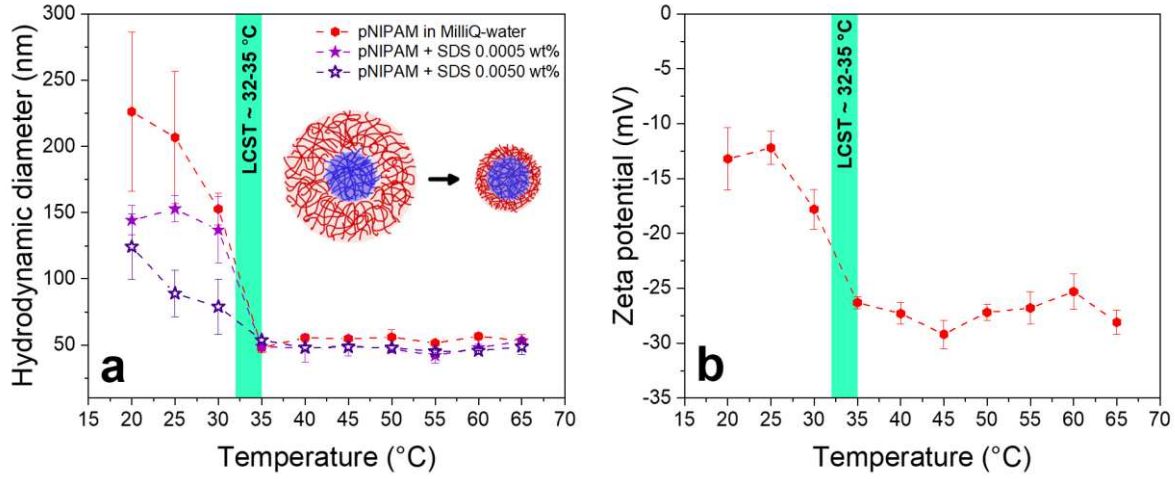

Figure 1. Hydrodynamic diameter of pNIPAM nanoparticles in Milli-Q water without and with SDS (a). Zeta potential of pNIPAM nanoparticles in Milli-Q water as a function of temperature (b). The green shaded region indicates the LCST region. The error bars are the standard deviation and lines are included to guide the eye.

The zeta potentials of pNIPAM nanoparticles in Milli-Q water were found to be slightly negative (Fig. 1b) which is likely attributed to the residual sulfate groups of the KPS initiator.[20] Below the LCST the zeta potential is c.a. −14 mV at 20°C and the magnitude increases to −27 mV above the LCST.[20, 28] The change in zeta potential correlates to the change in particle size,[18, 20, 23] with a reduced particle size increasing the surface density of exposed negative sulfate groups.[29]

Dynamic and steady state interfacial tensions. Figure 2 shows the dynamic and steady state interfacial tensions for heavy crude oil-water, with the aqueous phase containing either pNIPAM nanoparticles (Fig. 2a), SDS (Fig. 2b) or both (Fig. 2c). For pNIPAM only, the dynamic interfacial tension is found to strongly depend on the nanoparticle concentration, whereas the steady state ($\boldsymbol{t}$ > 1,000 s) interfacial tension does not, with $\boldsymbol{\sigma_\infty}$ ~14 mN/m, see also Fig. 3. For the dynamic interfacial tension, a three-step adsorption process best describes the changes: (i) particle diffusion to the crude oil-water interface; followed by (ii) diffusion-controlled interfacial adsorption (steps i and ii contribute to the observed time delay, when $\boldsymbol{\Delta\sigma}$ ~0 mN/m); and then (iii) forming hexagonal-packed arrays where the diffused-shells of the core-shell pNIPAM particles begin to interact. Further compression of the hexagonally-packed particle film can only be achieved by interpenetration of the diffused-shells. Eventually the particle film is sufficiently compressed that new particle adsorption ceases, hence, the steady state interfacial tension is independent of particle concentration.[17, 20] It should be noted that at the highest pNIPAM concentration (0.0050 wt%) no delay time was observed, and the interfacial tension was not observed to decrease from $\boldsymbol{\sigma_0}$ (~33.5 mN/m), due to the very fast interfacial partitioning of the nanoparticles (increased diffusion flux at higher concentrations) during expansion of the crude oil droplet.

For SDS only (Fig. 2b), the dynamic interfacial tension could not be accurately captured due to limitations relating to the rate of droplet generation and data capture. With the interfacial tension decreasing as the droplet is expanded, only the equilibrium interfacial tensions can be reliably compared. For increasing SDS concentration, the equilibrium interfacial tension decreases up to the cmc, σ_{cmc} = 5.8 mN/m (Fig. 3). When comparing the crude oil-water interfacial tension at an equivalent concentration of surface-active species (for example 0.0050 wt%), the reduced crude oil-water interfacial tension (-$\Delta\sigma$) is less for SDS than pNIPAM. However, the limiting (which is found at higher SDS concentrations up to the cmc) reduced crude oil-water interfacial tension can be lower with SDS than with pNIPAM, see Fig. 3.

Figure 2c shows the crude oil-water interfacial tensions for the pNIPAM + SDS blends (the total component concentrations are shown inset of Fig. 2c). When compared to the individual components, the time required for the interfacial tension to reach steady state is significantly longer (~4,000 s). At low total component concentrations (0.0005 and 0.001 wt%), the interfacial tension is more consistent with that of SDS-only, showing a weak time-dependency and the steady state interfacial tension within 9% of the SDS system, see grey boxes in Figs. 2e and 2f. At 0.0050 wt% pNIPAM + SDS (i.e. 0.0025 wt% pNIPAM + 0.0025 wt% SDS), the

behavior better resembles that of pNIPAM-only at an equivalent total component concentration, particularly when the two steady state interfacial tensions are compared, see green boxes in Figs. 2d and 2f (steady state interfacial tension within 18% of the pNIPAM system). However, while the steady state system better resembles that of pNIPAM-only, the dynamic interfacial tension is significantly slowed. Such behavior is likely justified by a two-stage absorption process, where SDS first rapidly adsorbs at the oil-water interface, but is then gradually displaced by the pNIPAM nanoparticles with increasing time.

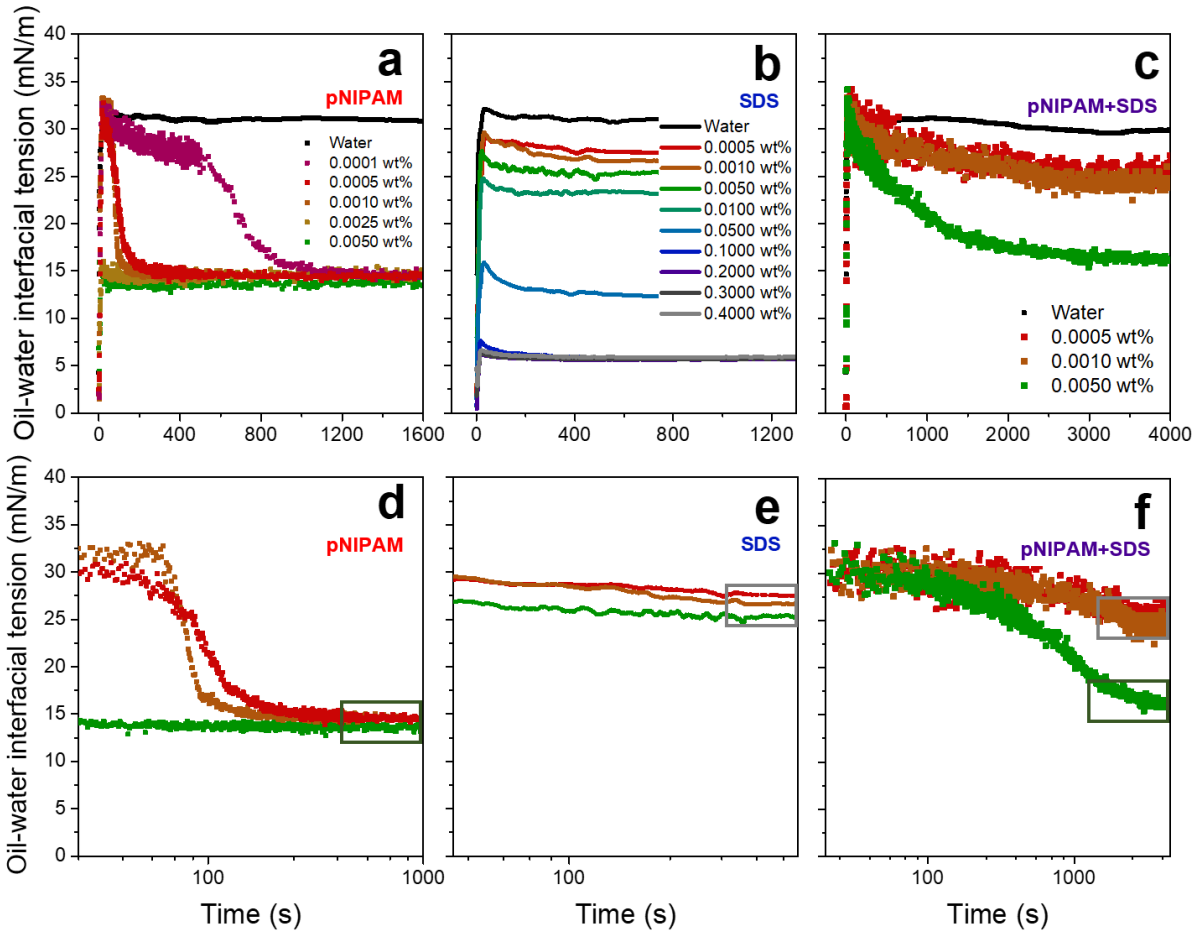

Figure 2. Dynamic oil-water interfacial tensions at 60 °C for pNIPAM (a), SDS (b) and pNIPAM + SDS blend (c). Equivalent data shown as semi-log plots (d) – (f). Similarities between the pNIPAM + SDS blend and the individual components are highlighted by the colored boxes.

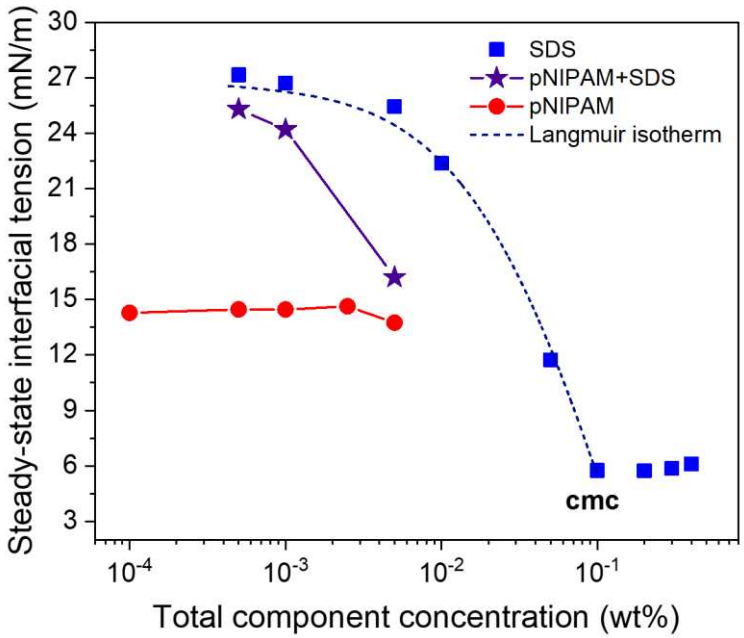

Figure 3. Comparing the steady state crude oil-water interfacial tensions as a function of total component concentration: pNIPAM, SDS and pNIPAM + SDS blend. All data is collected at 60 °C. The dashed line is the Langmuir isotherm fit of the SDS data, and the red and purple solid lines are added to guide the eye.

With pNIPAM nanoparticles irreversibly adsorbed at the oil-water interface (see discussion below), the short-time response to particle adsorption can be first analyzed using the Ward-Tordai equation for diffusion-controlled adsorption:[30-31]

$$\Gamma_t = 2\sqrt{\frac{D_{WT}}{\pi}}C_0\sqrt{t} \qquad (1)$$

where Γ_t is taken to be the interfacial concentration of pNIPAM at time t, D_{WT} is the particle interfacial diffusion coefficient from the bulk to the interface and C_0 is the particle concentration. The interfacial concentration (Γ_t) relates to the surface pressure ($\sigma_0 - \sigma_t$) by:

$$\sigma_0 - \sigma_t = \Gamma_t N_A k_B T \qquad (2)$$

where N_A is the Avogadro's constant and k_B the Boltzmann constant. Combining Eqs. 1 and 2, the relationship for the time-dependent interfacial tension is given by:

$$\sigma_t = \sigma_0 - 2N_A k_B T\sqrt{\frac{D_{WT}}{\pi}}C_0\sqrt{t} \qquad (3)$$

and according to Eq. 3, σ_t is proportional to $\sqrt{t}$ for a diffusion-controlled process. The slope k which is determined from σ_t versus $\sqrt{t}$ should then be proportional to the bulk particle concentration (C_0) which is given by:

$$k = 2N_A k_B T \sqrt{\frac{D_{WT}}{\pi}} C_0. \quad (4)$$

From analyzing the data for t < ~200 s (Fig. S2), it was found that k is directly proportional to C_0 for both pNIPAM and the pNIPAM + SDS blend, see Fig. S3. Hence for both systems, the initial stage of particle adsorption is diffusion-controlled. From Eq. 4, the interfacial diffusion coefficient (D_{WT}), which describes particle diffusion from the interfacial boundary layer to the oil-water interface, can then be calculated. For the pNIPAM + SDS blend, D_{WT} is an apparent interfacial diffusion coefficient as SDS rapidly adsorbs (adsorption occurs during drop creation) to hinder pNIPAM adsorption. It is worth noting that D_{WT} does not account for in-plane particle diffusion at the oil-water interface.[32-33]

Furthermore, others have described the initial stage of nanoparticle adsorption by accounting for the particle detachment energy (E), with the modified Ward-Tordai equation given as:[34-35]

$$k = 2N_A E \sqrt{\frac{D_{WT*}}{\pi}} C_0 \quad (5)$$

where D_{WT*} is the particle interfacial diffusion coefficient. The energy required to remove a particle from the crude oil-water interface can be calculated using, $E = \pi a^2 \sigma_{OW}(1 \pm cos\theta)^2$,[36] where a is the particle radius, σ_{OW} the oil-water interfacial tension, and θ the oil-water-particle three-phase contact angle. Using the measured values of a = 55 nm, σ_{OW} = 33.5 N/m and θ = 30°,[37] the particle detachment energy is E ~1,242 $k_B T$, which given the fact that the thermal energy is approximately $50k_B T$,[34] the pNIPAM particles are correctly assumed to be irreversibly adsorbed at the oil-water interface. Furthermore, pNIPAM is a 'soft' particle that can deform at the oil-water interface, thus increasing its apparent size, anchoring the particle even more strongly to the oil-water interface.[38]

Finally, the particle bulk diffusion coefficient (D_{Bulk_SE}) can be calculated from the Stokes-Einstein equation, which is given by:[39]

$$D_{Bulk\_SE} = \frac{k_B T}{6\pi\mu R_h} \quad (6)$$

where R_h is the particle hydrodynamic radius and μ the fluid viscosity. All three calculated diffusion coefficients (D_{WT}, D_{WT^*} and D_{Bulk_SE}) are summarized in Table 2.

By comparing the two interfacial diffusion coefficients, D_{WT} is much greater than D_{WT^*} at an equivalent total component concentration because E is much greater than k_BT, see Eqs. 4 and 5. Since the modified Ward-Tordai equation (Eq. 5) accounts for the interfacial diffusion coefficient of particles rather than small molecules, the interfacial diffusion coefficients from Eq. 4 are likely to be inaccurate, and is consistent with observations previously reported.[34]

Table 2. Comparison of diffusion coefficients: $\boldsymbol{D_{WT}}$, $\boldsymbol{D_{WT^*}}$ and $\boldsymbol{D_{Bulk\_SE}}$.

Total component concentration (wt%)	**Interfacial diffusion coefficient (Ward-Tordai)**		**Interfacial diffusion coefficient (Modified Ward-Tordai)**		**Bulk diffusion coefficient (Stokes-Einstein)**	
	D_{WT} ($mol^2/m^4 \cdot s$)	**Normalized D_{WT}[a]**	**D_{WT^*} ($mol^2/m^4 \cdot s$)**	**Normalized D_{WT^*}[a]**	**D_{Bulk_SE} (m^2/s)**	**Normalized D_{Bulk_SE}[a]**
pNIPAM in Milli-Q water						
0.0001	64	0.0732	4.14×10^{-9}	0.0732	1.85×10^{-11}	1.00
0.0005	428	0.4906	2.77×10^{-8}	0.4906	1.85×10^{-11}	1.00
0.0010	804	0.9222	5.21×10^{-8}	0.9222	1.85×10^{-11}	1.00
0.0025	872	1.0000	5.65×10^{-8}	1.0000	1.85×10^{-11}	1.00
0.0050	*Undetermined due to infinite slope k*				1.85×10^{-11}	1.00
pNIPAM + SDS in Milli-Q water						
0.0005	0.456	0.0005	2.96×10^{-11}	0.0005	1.85×10^{-11}	1.00
0.0010	0.188	0.0002	1.22×10^{-11}	0.0002	2.18×10^{-11}	1.18
0.0050	0.067	0.0001	4.32×10^{-12}	0.0001	2.29×10^{-11}	1.24

[a] D is normalized by highest D at a total component concentration of 0.0025 wt% in Milli-Q water.

Since the unit of C_0 is wt% and not mol/m^3, a direct comparison between the particle interfacial diffusion coefficient and particle bulk diffusion coefficient can only be made when normalizing the diffusion coefficients to that at a selected total component concentration.[18, 31] For pNIPAM-only, the values of D_{Bulk_SE} are independent of the component concentration, as is described by Eq. 6. However, for the pNIPAM + SDS blend, the value of D_{Bulk_SE} increases slightly with increasing total component concentration, which can be attributed to the enhanced dispersion of the pNIPAM particles with SDS, see Fig. 1a.

For pNIPAM-only, the interfacial diffusion coefficients were found to strongly depend on the total component concentration, increasing with higher particle concentrations. However, for the pNIPAM + SDS blend, the interfacial diffusion coefficients were significantly smaller than pNIPAM-only. The apparent interfacial diffusion coefficient was less dependent on the total

component concentration and decreased with increasing concentration. Since SDS rapidly adsorbs, the apparent interfacial diffusion coefficients reflect that of pNIPAM, and it becomes clear that the presence of SDS hinders adsorption of pNIPAM at the oil-water interface. Such behavior would support a two-step adsorption process.

Interfacial dominant-region map. For the blended system, it is clear that the two components are interfacially active, but their presence at the interface depends on the total component concentration and adsorption time. Based on the previous discussion, the short-time behavior is influenced by adsorbing SDS which will affect adsorption of pNIPAM nanoparticles, which for the total component concentrations considered (up to 0.0050 wt%), are found to be more strongly interfacially active than SDS, see Fig. 3.

Referring back to Fig. 2, the competition between the two components to partition at the crude oil-water interface is highlighted from the short-time and long-time dynamics (Fig. 2f). For example, at a total component concentration of 0.0050 wt%, the short-time behavior better resembles that of SDS-only, since for pNIPAM-only the interfacial tension is significantly lower. Due to its smaller molecule size compared to pNIPAM nanoparticles, faster adsorption by SDS is reasonable with a typical diffusion coefficient of ~1×10^{-11} m^2/s.[40-41] However, at longer time intervals (t >100 s) the interfacial tension begins to decrease, not consistent with SDS-only, and so would support the displacement of SDS by pNIPAM nanoparticles, since the steady state interfacial tension for pNIPAM is lower than SDS. Given sufficient time (t > 3,000 s), the interfacial tension of the pNIPAM + SDS blend becomes almost equivalent to pNIPAM-only, suggesting the significant adsorption of pNIPAM particles.

At lower total component concentrations (0.0005 and 0.0010 wt%), the short-time dynamic would be consistent with SDS adsorption, but the longer time dynamic is less conclusive and is likely to be a mixed interface of SDS and pNIPAM since the steady state interfacial tension is between that of the two individual components at an equivalent concentration.

Figure 4 compares the reduced interfacial tensions ($-\Delta\sigma = \sigma_0 - \sigma$) for the individual and blended systems at steady state and time intervals of 1,000 and 2,000 s (only for the blended system). At low total component concentrations, the behavior is more SDS-like (blue shading), but at the highest total component concentration the steady state interfacial tension is more pNIPAM-like (red shading), which progressively transitions from more SDS-like with increasing adsorption time.

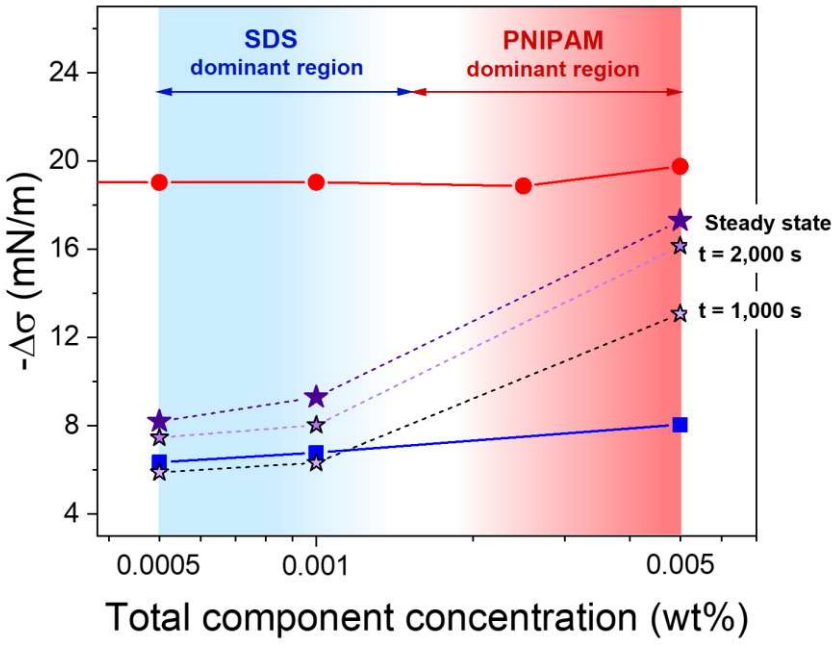

Figure 4. Reduced interfacial tensions ($-\Delta\sigma = \sigma_0 - \sigma$) for SDS (blue square), pNIPAM (red circle) and pNIPAM + SDS (purple stars) as a function of the total component concentration. σ_0 is taken to be 33.5 mN/m for the pristine interface. Blue color shading defines the region more SDS-like and the red color shading the region more pNIPAM-like. Individual component (pNIPAM or SDS) concentration is diluted by a factor of 2. The lines are added to guide the eye.

As a first-order approximation, the contribution of SDS and pNIPAM to lowering the interfacial tension can be taken as a weighted-arithmetic mean of the steady state interfacial tensions of each individual component, thus approximating the surface-active contribution of both SDS and pNIPAM ($A_{PNIPAM+SDS}$). For the blend (pNIPAM + SDS), the increase in $-\Delta\sigma$ ($-\Delta\sigma_{PNIPAM+SDS}$) is given by the summation of both components (A_i) and the individual $-\Delta\sigma_i$:

$$-\Delta\sigma_{PNIPAM+SDS} = \frac{\sum_{i=1}^{n} -\Delta\sigma_i A_i}{\sum_{i=1}^{n} A_i} \tag{7}$$

$$-\Delta\sigma_{PNIPAM+SDS} = \frac{-\Delta\sigma_{PNIPAM} A_{PNIPAM} + -\Delta\sigma_{SDS} A_{SDS}}{A_{PNIPAM+SDS}} \tag{8}$$

For a two-component blend, the surface-active contribution ($A_{PNIPAM+SDS}$) equals one as it is the combined contribution of each component ($A_{PNIPAM+SDS} \approx A_{PNIPAM} + A_{SDS} = 1$), thus Eq. 8 becomes:

$$-\Delta\sigma_{PNIPAM+SDS} = \frac{-\Delta\sigma_{PNIPAM}(1 - A_{SDS}) + -\Delta\sigma_{SDS} A_{SDS}}{1} \tag{9}$$

The surface-active contribution of each component (A_i) partitioned at the crude oil-water interface is determined from Eq. 9, which assumes no interactions between the two components. From Eq. 9, the changing surface-active contributions of pNIPAM (Fig. 5a) and SDS (Fig. 5b) dependent on time and the total component concentration of the blend are shown in Fig. 5. At the highest total component concentration, pNIPAM is predominantly partitioned at the crude oil-water interface, while at the lowest total component concentrations SDS does, see Fig. 5c. It is shown with interfacial aging time that the surface-active contribution of pNIPAM increases at all total component concentrations and does so by removing the initially adsorbed SDS. Such behavior can be justified based on the relative differences in bulk diffusion coefficients (SDS > pNIPAM) and the lowest interfacial tensions (pNIPAM > SDS) for the component concentrations studied. To clarify this behavior, a series of tests were run where SDS and pNIPAM were sequentially added to the aqueous phase once one component had reached steady state (Fig. S4 in the Supporting Information). At the lowest total component concentration (0.0005 wt%), when adding the second component the interfacial tension remained almost unchanged. When the total component concentration was increased by an order of magnitude, the decrease in interfacial tension by adding SDS following pNIPAM was negligible compared to the significant reduction of ~5.5 mN/m when pNIPAM was added following SDS, thus confirming its ability to displace SDS at partition at the crude oil-water interface.

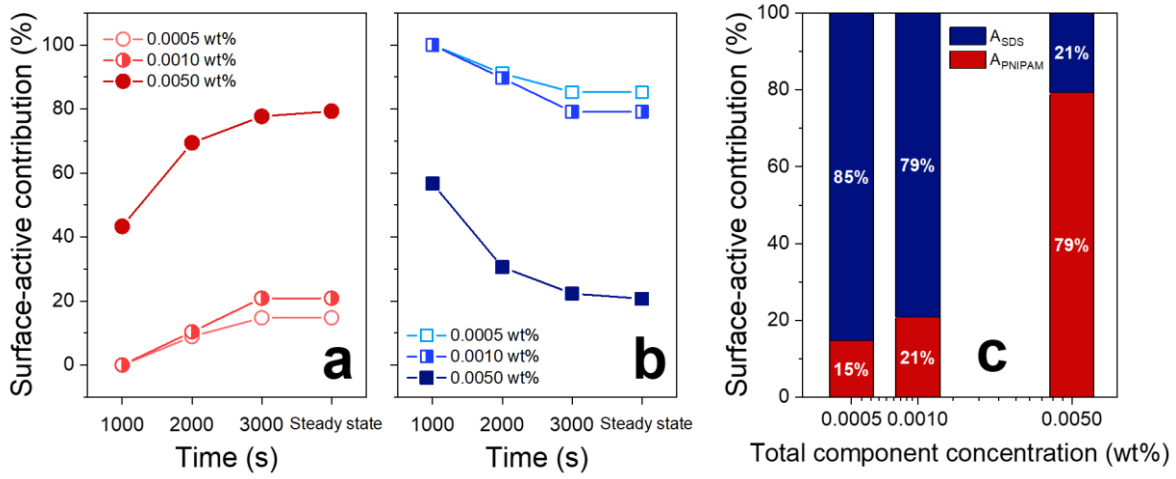

Figure 5. Surface-active contributions of (a) pNIPAM (A_{PNIPAM}) and (b) SDS (A_{SDS}) in the pNIPAM + SDS blend as a function of interfacial aging time and the total component concentration. Steady state values are compared in (c). Individual component (pNIPAM or SDS) concentration is diluted by a factor of 2. Lines are added to guide the eye.

Conclusion

A two-component (pNIPAM and SDS) aqueous fluid has been studied to reduce the interfacial tension of a crude oil-water interface. While the findings are broadly applicable to multiphase fluids with multiple surface-active species, the interest here was to study fluids that have potential application to enhance recovery of crude oil. The main conclusions from the study are:

1. Both the anionic surfactant, SDS, and the negatively charged nanoparticles, pNIPAM, adsorb at the crude oil-water interface to lower its interfacial tension.
2. Adding SDS improved the dispersion of pNIPAM nanoparticles by increased electrostatic repulsion, and at the concentrations studied, did not modify the pNIPAM LCST.
3. With a lower molecular weight, SDS could rapidly adsorb at the crude oil-water interface. However, the pNIPAM nanoparticles were more strongly interfacially active when the component concentration was less than 0.0050 wt%.
4. When mixed together, a two-step adsorption process was observed. At high total component concentration (0.0050 wt%), SDS initially adsorbs but is then displaced by the slower diffusing but more interfacially active pNIPAM. At steady state, the interfacial tension approximates to a more pNIPAM-like saturated interface. For lower total component concentrations, the same dynamics occur, but the interface remains more SDS-like.

Overall, the study highlights the potential use of pNIPAM as an additive to enhance oil recovery. Furthermore, its characteristic ‘switchable’ property makes it ideal for destabilizing emulsions, something that is more challenging to do with surfactant-stabilized emulsions. Future fluids for EOR should consider the use of responsive particles to overcome several significant limitations of current practices.

Supporting Information

S1. Solution conductivity; S2. Slope (k) determination during initial adsorption; S3. Two component consecutive addition.

Acknowledgement

Financial support for this work is greatly acknowledged with contributions from Chiang Mai University, and China Scholarship Council (No. 201906440066) (J.J.). The authors would like to thank Anton Paar Ltd. (UK) for use of the high temperature density meter.

References

1. Zhang, H.; Nikolov, A.; Wasan, D., Enhanced Oil Recovery (EOR) Using Nanoparticle Dispersions: Underlying Mechanism and Imbibition Experiments. *Energy & Fuels* **2014,** *28* (5), 3002-3009.
2. Suleimanov, B. A.; Ismailov, F. S.; Veliyev, E. F., Nanofluid for enhanced oil recovery. *Journal of Petroleum Science and Engineering* **2011,** *78* (2), 431-437.
3. Rezk, M. Y.; Allam, N. K., Impact of Nanotechnology on Enhanced Oil Recovery: A Mini-Review. *Industrial & Engineering Chemistry Research* **2019,** *58* (36), 16287-16295.
4. Tangparitkul, S.; Charpentier, T.; Pradilla, D.; Harbottle, D., Interfacial and Colloidal Forces Governing Oil Droplet Displacement: Implications for Enhanced Oil Recovery. *Colloids and Interfaces* **2018,** *2* (3), 30.
5. Fan, H.; Striolo, A., Nanoparticle effects on the water-oil interfacial tension. *Physical Review E* **2012,** *86* (5), 051610.
6. Zhang, H.; Ramakrishnan, T.; Nikolov, A.; Wasan, D., Enhanced oil displacement by nanofluid's structural disjoining pressure in model fractured porous media. *Journal of colloid and interface science* **2018,** *511*, 48-56.
7. Lim, S.; Horiuchi, H.; Nikolov, A. D.; Wasan, D., Nanofluids Alter the Surface Wettability of Solids. *Langmuir* **2015,** *31* (21), 5827-5835.
8. Lim, S.; Zhang, H.; Wu, P.; Nikolov, A.; Wasan, D., The dynamic spreading of nanofluids on solid surfaces – Role of the nanofilm structural disjoining pressure. *Journal of Colloid and Interface Science* **2016,** *470*, 22-30.
9. Choi, S. K.; Son, H. A.; Kim, H. T.; Kim, J. W., Nanofluid Enhanced Oil Recovery Using Hydrophobically Associative Zwitterionic Polymer-Coated Silica Nanoparticles. *Energy & Fuels* **2017,** *31* (8), 7777-7782.
10. Yusuf, M.; Wathon, M. H.; Thanasaksukthawee, V.; Saul, A.; Tangparitkul, S., Adsorption of Saponin Natural Surfactant on Carbonate Rock and Comparison to Synthetic Surfactants: An Enhanced Oil Recovery Prospective. *Energy & Fuels* **2021,** *35* (14), 11193-11202.
11. Yang, Y.; Peng, W.; Zhang, H.; Wang, H.; He, X., The oil/water interfacial behavior of microgels used for enhancing oil recovery: A comparative study on microgel powder and microgel emulsion. *Colloids and Surfaces A: Physicochemical and Engineering Aspects* **2022,** *632*, 127731.
12. Zhou, Y.; Luo, Z.; Xu, M.; Zhao, T.; Ma, X.; Zhou, S.; Wen, B.; Yang, D., Preparation and Properties of Temperature-Sensitive P(NIPAM-AM) Nano–Microspheres in Enhanced Oil Recovery. *Energy & Fuels* **2023,** *37* (1), 204-213.
13. Ni, C.; Wang, Y.; Hou, Q.; Li, X.; Zhang, Y.; Wang, Y.; Xu, Y.; Zhao, Y., Phase transformation of thermoresponsive surfactant triggered by its concentration and temperature. *Journal of Petroleum Science and Engineering* **2020,** *193*, 107410.
14. Pichot, R.; Spyropoulos, F.; Norton, I. T., Competitive adsorption of surfactants and hydrophilic silica particles at the oil–water interface: Interfacial tension and contact angle studies. *Journal of Colloid and Interface Science* **2012,** *377* (1), 396-405.

15. Ravera, F.; Santini, E.; Loglio, G.; Ferrari, M.; Liggieri, L., Effect of Nanoparticles on the Interfacial Properties of Liquid/Liquid and Liquid/Air Surface Layers. *The Journal of Physical Chemistry B* **2006,** *110* (39), 19543-19551.
16. Smits, J.; Vieira, F.; Bisswurn, B.; Rezwan, K.; Maas, M., Reversible Adsorption of Nanoparticles at Surfactant-Laden Liquid–Liquid Interfaces. *Langmuir* **2019,** *35* (34), 11089-11098.
17. Li, Z.; Richtering, W.; Ngai, T., Poly(N-isopropylacrylamide) microgels at the oil-water interface: temperature effect. *Soft Matter* **2014,** *10* (33), 6182-6191.
18. Li, Z.; Harbottle, D.; Pensini, E.; Ngai, T.; Richtering, W.; Xu, Z., Fundamental Study of Emulsions Stabilized by Soft and Rigid Particles. *Langmuir* **2015,** *31* (23), 6282-6288.
19. Destribats, M.; Lapeyre, V.; Wolfs, M.; Sellier, E.; Leal-Calderon, F.; Ravaine, V.; Schmitt, V., Soft microgels as Pickering emulsion stabilisers: role of particle deformability. *Soft Matter* **2011,** *7* (17), 7689-7698.
20. Li, Z.; Geisel, K.; Richtering, W.; Ngai, T., Poly (N-isopropylacrylamide) microgels at the oil–water interface: adsorption kinetics. *Soft Matter* **2013,** *9* (41), 9939-9946.
21. Barnes, G.; Gentle, I., *Interfacial science: an introduction*. Oxford University Press: 2011.
22. Schild, H. G., Poly(N-isopropylacrylamide): experiment, theory and application. *Progress in Polymer Science* **1992,** *17* (2), 163-249.
23. Pelton, R., Temperature-sensitive aqueous microgels. *Advances in colloid and interface science* **2000,** *85* (1), 1-33.
24. Chen, J.; Gong, X.; Yang, H.; Yao, Y.; Xu, M.; Chen, Q.; Cheng, R., NMR Study on the Effects of Sodium n-Dodecyl Sulfate on the Coil-to-Globule Transition of Poly(N-isopropylacrylamide) in Aqueous Solutions. *Macromolecules* **2011,** *44* (15), 6227-6231.
25. Schild, H. G.; Tirrell, D. A., Interaction of poly(N-isopropylacrylamide) with sodium n-alkyl sulfates in aqueous solution. *Langmuir* **1991,** *7* (4), 665-671.
26. Chen, J.; Xue, H.; Yao, Y.; Yang, H.; Li, A.; Xu, M.; Chen, Q.; Cheng, R., Effect of Surfactant Concentration on the Complex Structure of Poly(N-isopropylacrylamide)/Sodium n-Dodecyl Sulfate in Aqueous Solutions. *Macromolecules* **2012,** *45* (13), 5524-5529.
27. Wang, X.; Li, L., How does the anionic surfactant SDS affect the association of hydrophobically end-modified PNIPAM chains in aqueous solution? *Polymer* **2016,** *88*, 123-132.
28. Daly, E.; Saunders, B. R., Temperature-dependent electrophoretic mobility and hydrodynamic radius measurements of poly(N-isopropylacrylamide) microgel particles: structural insights. *Physical Chemistry Chemical Physics* **2000,** *2* (14), 3187-3193.
29. Utashiro, Y.; Takiguchi, M.; Satoh, M., Zeta potential of PNIPAM microgel particles dispersed in water—effects of charged radical initiators vs. OH− ion adsorption. *Colloid and Polymer Science* **2017,** *295* (1), 45-52.
30. Ward, A. F. H.; Tordai, L., Time-Dependence of Boundary Tensions of Solutions I. The Role of Diffusion in Time-Effects. *The Journal of Chemical Physics* **1946,** *14* (7), 453-461.
31. Bhushan, B.; Nosonovsky, M.; Jung, Y. C., Towards optimization of patterned superhydrophobic surfaces. *Journal of the Royal Society Interface* **2007,** *4* (15), 643-648.
32. Cohin, Y.; Fisson, M.; Jourde, K.; Fuller, G. G.; Sanson, N.; Talini, L.; Monteux, C., Tracking the interfacial dynamics of PNiPAM soft microgels particles adsorbed at the air–water interface and in thin liquid films. *Rheologica Acta* **2013,** *52* (5), 445-454.
33. Tarimala, S.; Ranabothu, S. R.; Vernetti, J. P.; Dai, L. L., Mobility and In Situ Aggregation of Charged Microparticles at Oil−Water Interfaces. *Langmuir* **2004,** *20* (13), 5171-5173.

34. Bizmark, N.; Ioannidis, M. A.; Henneke, D. E., Irreversible adsorption-driven assembly of nanoparticles at fluid interfaces revealed by a dynamic surface tension probe. *Langmuir* **2014,** *30* (3), 710-717.
35. Hua, X.; Frechette, J.; Bevan, M. A., Nanoparticle adsorption dynamics at fluid interfaces. *Soft Matter* **2018,** *14* (19), 3818-3828.
36. Binks, B. P., Particles as surfactants—similarities and differences. *Current Opinion in Colloid & Interface Science* **2002,** *7* (1), 21-41.
37. Geisel, K.; Isa, L.; Richtering, W., Unraveling the 3D Localization and Deformation of Responsive Microgels at Oil/Water Interfaces: A Step Forward in Understanding Soft Emulsion Stabilizers. *Langmuir* **2012,** *28* (45), 15770-15776.
38. Style, R. W.; Isa, L.; Dufresne, E. R., Adsorption of soft particles at fluid interfaces. *Soft Matter* **2015,** *11* (37), 7412-7419.
39. Berne, B. J.; Pecora, R., *Dynamic light scattering: with applications to chemistry, biology, and physics*. Courier Corporation: 2000.
40. Kinoshita, K.; Parra, E.; Needham, D., Adsorption of ionic surfactants at microscopic air-water interfaces using the micropipette interfacial area-expansion method: Measurement of the diffusion coefficient and renormalization of the mean ionic activity for SDS. *Journal of Colloid and Interface Science* **2017,** *504*, 765-779.
41. Collura, J. S.; Harrison, D. E.; Richards, C. J.; Kole, T. K.; Fisch, M. R., The Effects of Concentration, Pressure, and Temperature on the Diffusion Coefficient and Correlation Length of SDS Micelles. *The Journal of Physical Chemistry B* **2001,** *105* (21), 4846-4852.

Graphical Abstract